Available online at www.sciencedirect.com

SCIENCE DIRECT®

Polyhedron 25 (2006) 1737–1746

POLYHEDRON

www.elsevier.com/locate/poly

4-(Hydroxymethyl)pyridine and pyrimidine in manganese benzoate chemistry: Preparation and characterization of hexanuclear clusters featuring the $\{Mn_4^{II}Mn_2^{III}(\mu_4\text{-}O)_2\}^{10+}$ core

Theocharis C. Stamatatos [a,b], Dolos Foguet-Albiol [c], Spyros P. Perlepes [a], Catherine P. Raptopoulou [d], Aris Terzis [d], Costas S. Patrickios [b], George Christou [c,*], Anastasios J. Tasiopoulos [b,*]

[a] *Department of Chemistry, University of Patras, GR 265 04 Patras, Greece*
[b] *Department of Chemistry, University of Cyprus, 1678 Nicosia, Cyprus*
[c] *Department of Chemistry, University of Florida, Gainesville, FL 32611 7200, USA*
[d] *Institute of Materials Science, NCSR "Demokritos", GR 153 10 Aghia Paraskevi Attikis, Greece*

Received 15 October 2005; accepted 14 November 2005
Available online 27 December 2005

Abstract

The use of 4-(hydroxymethyl)pyridine (4hmpH) and pyrimidine (pym) in manganese benzoate chemistry has been investigated. The reactions of 4hmpH and pym with $Mn(O_2CPh)_2 \cdot 2H_2O$ in MeCN affords the complexes $[Mn_6O_2(O_2CPh)_{10}(4hmpH)_3(MeCN)]$ (**1**) and $[Mn_6O_2(O_2CPh)_{10}(pym)_2(MeCN)_2]$ (**2**), respectively. Complex **1** contains a $\{Mn_6O_2\}^{10+}$ core that can be conveniently described as two edge-sharing Mn_4 tetrahedra at the center of each of which is a μ_4-O^{2-} ion. Peripheral ligation to the octahedrally coordinated Mn centres is provided by 10 bridging $PhCO_2^-$ ligands, three N-monodentate ligands and one terminal MeCN group. The complex is mixed-valence ($Mn_4^{II}Mn_2^{III}$) and the Mn^{III} ions are assigned as the two central metal centres bridged by two O^{2-} ions. The molecular structure of **2** is very similar to that of **1**, except that the terminal ligands are two monodentate pym molecules and two MeCN groups. IR data are discussed in terms of the nature of bonding and the known structures. Complexes **1** and **2** were characterized by variable-temperature ac and dc magnetic susceptibility data and found to possess a total spin ground state of 0. The $S_T = 0$ ground state is explained in terms of the strong antiferromagnetic coupling within the central $Mn_2^{III}O_2$ unit.

Keywords: Crystal structures; 4-(Hydroxymethyl)pyridine metal complexes; Magnetochemistry; Manganese benzoate chemistry; Mixed-valence manganese clusters; Pyrimidine manganese complexes

1. Introduction

The current intense interest in the synthetic and physical studies of new manganese carboxylate clusters has two main driving forces: (i) the desire to recreate with synthetic models the structure, spectroscopic properties and/or function of the active site of metalloenzymes containing a carboxylate-bridged manganese core such as the water oxidizing complex of photosystem II [1]; and (ii) the realization that Mn carboxylate clusters often exhibit high-spin ground states as a result of ferromagnetic exchange interactions and/or spin frustration effects [2]. In addition, such clusters have provided the first and most studied examples of molecular species that can function as nanoscale magnetic particles at very low temperatures. These complexes have been named single-molecule magnets (SMMs) [3,4] to reflect the fact that their magnetic properties are due to a combination of two intramolecular properties (and

---

* Corresponding authors. Tel.: +1 352 392 6737, fax: +1 352 392 8757 (G. Christou); Tel.: +357 22892765, fax: +357 22892801 (A.J. Tasiopoulos).

E-mail addresses: christou@chem.ufl.edu (G. Christou), atasio@ucy.ac.cy (A.J. Tasiopoulos).

0277-5387/$ - see front matter © 2005 Elsevier Ltd. All rights reserved.
doi:10.1016/j.poly.2005.11.019

not to intermolecular exchange interactions and long-range ordering), namely a high-spin ground state and a large magnetoanisotropy, the latter reflected in a large and negative value of the zero-field splitting parameter, D.

The future health of the field of high-spin molecules and the chances of identifying new SMMs will both benefit from the development of new synthesis methodologies to Mn carboxylate clusters [5]. Discovering new preparative routes is thus of great interest not only for the isolation of completely new complexes but also as a means of building up families of related Mn carboxylate species so that structure–property relations can be developed. The choice of ligands in such studies is obviously crucial, because the hapticity, flexibility, chelate bite size(s) and other ligand properties are of paramount importance in determining the structure of the product.

One synthetic methodology that has proven to be very useful for the synthesis of new polynuclear Mn complexes is the reaction of a chelating ligand with simple Mn carboxylate sources, e.g., $Mn(O_2CMe)_2 \cdot 4H_2O$ and $Mn(O_2CPh)_2 \cdot 2H_2O$, or with a preformed Mn carboxylate cluster that does not already incorporate any chelating ligands [6]. Some of the most successful starting materials employed for this purpose are the trinuclear $[Mn_3O(O_2CR)_6(py)_3]^{n+}$ ($n = 0$, 1; py = pyridine) complexes [7] and the tetranuclear cluster $(NBu^n_4)[Mn_4O_2(O_2CPh)_9(H_2O)]$ [8], which have afforded many new complexes with a variety of nuclearities. Ligands that have previously proven to be useful in these syntheses are, amongst others, 2,2′-bipyridine [9], 2-picolinate [10] and the anion of dibenzoylmethane [11]. The presence of a chelating ligand was found to have profound effects on the nuclearity and metal topology of the resultant product. Thus, for example, the reaction of 2,2′-bipyridine (bpy) with $[Mn_3O(O_2CR)_6(py)_3]^+$ was the original way by which the tetranuclear "butterfly" complexes $[Mn_4O_2(O_2CR)_7(bpy)_2]^+$ were obtained [9a].

A potentially powerful [12] but barely explored route to new Mn carboxylate compounds is the use of bis(monodentate) bridging ligands in place of traditional bidentate chelating ligands. The advantages of bis(monodentate) bridging ligands include (i) the possible diversion of known reaction systems developed using chelating ligands to new species as a result of the different ligation mode of the bridging ligands, (ii) the possibility of triggering aggregation of preformed species into new, higher nuclearity products, and (iii) the potential of linking cluster units to form coordination polymers.

The organic ligands 4-(hydroxymethyl)pyridine (4hmpH) and pyrimidine (pym), see Fig. 1, seemed attractive to us for the above applications. Contrary to its 2-(hydroxymethyl)pyridine isomer [2,4e,13], there are no structures of Mn compounds containing 4hmpH in the literature. The use of pym in Mn chemistry has been confined to few mononuclear and polymeric complexes [14]. Our own work with these ligands has now led to the preparation of two hexanuclear, mixed-valence Mn benzoate clusters. The syntheses, structures and physical properties of the products are described.

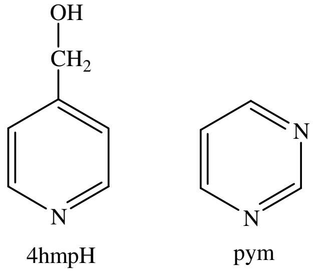

Fig. 1. The ligands used in this work.

2. Experimental

2.1. General and physical measurements

All manipulations were performed under aerobic conditions using materials (reagent grade) and solvents as received. $Mn(O_2CPh)_2 \cdot 2H_2O$ was prepared as described elsewhere [8].

Microanalyses (C, H, N) were performed by the in-house facilities of the Chemistry Department at the University of Florida. IR spectra (4000–450 cm^{-1}) were recorded on a Perkin–Elmer 16 PC FC spectrometer with samples prepared as KBr pellets. Magnetic susceptibility measurements were carried out for polycrystalline samples of complexes **1** and **2** (vide infra) in the range 1.8–300 K using a Quantum Design MPMS SQUID magnetometer; the applied magnetic field was 0.1 T. Diamagnetic corrections were applied to the observed paramagnetic susceptibilities using Pascal's constants.

2.2. Compound preparation

2.2.1. $[Mn_6O_2(O_2CPh)_{10}(4hmpH)_3(MeCN)] \cdot 2MeCN$ (*1* · 2MeCN)

A colourless solution of $Mn(O_2CPh)_2 \cdot 2H_2O$ (0.17 g, 0.5 mmol) in MeCN (15 ml) was treated with solid 4hmpH (0.05 g, 0.5 mmol). The solid soon dissolved. The resulting pale yellow solution was stirred for about 2 h, during which time the reaction mixture colour changed from pale yellow to deep orange. A small quantity of undissolved material was removed by filtration and the filtrate layered with Et_2O (30 ml). After several days, large orange prisms formed; they were collected by filtration, washed with Et_2O and dried in air. Yield: 60% (based on the total available Mn). The dried sample analysed as solvent-free. *Anal.* Calc. for $C_{90}H_{74}N_4O_{25}Mn_6$: C, 55.7; H, 3.9; N, 2.9. Found: C, 55.9; H, 3.8; N, 3.0%. Selected IR data (KBr pellet, cm^{-1}): 3413mb, 1602s, 1563s, 1492m, 1400s, 1304w, 1227w, 1176m, 1097w, 1069m, 1025m, 941w, 841m, 718s, 676m, 610m, 560w, 471m, 418w.

2.2.2. $[Mn_6O_2(O_2CPh)_{10}(pym)_2(MeCN)_2]$ (**2**)

A colourless solution of $Mn(O_2CPh)_2 \cdot 2H_2O$ (0.13 g, 0.4 mmol) in MeCN (15 ml) was added to a solution of pym (0.06 ml, 0.8 mmol) in the same solvent (5 ml). The resulting yellow solution was stirred for about 3 h, during which time the reaction mixture colour changed from yellow to deep orange. A small quantity of undissolved material was removed by filtration and the filtrate was allowed to stand undisturbed at room temperature. After several days, large orange prisms formed; they were collected by filtration, washed with Et_2O and dried in vacuo over silica gel. Yields as high as 55% were obtained (based on the Mn content). *Anal.* Calc. for $C_{82}H_{64}N_6O_{22}Mn_6$: C, 54.3; H, 3.6; N, 4.6. Found: C, 54.5; H, 3.5; N, 4.7%. Selected IR data (KBr pellet, cm^{-1}): 3065 m, 1606s, 1568s, 1490m, 1467m, 1447m, 1396s, 1305w, 1228m, 1175m, 1069m, 1024m, 1005w, 936w, 841m, 715s, 674m, 635m, 607s, 557w, 460m, 425w.

2.3. Single-crystal X-ray crystallography

Crystals of **1** · 2MeCN and **2** were mounted in capillary and in a glass fibre covered with epoxy glue, respectively. Diffraction measurements were made on a Crystal Logic Dual Goniometer diffractometer using graphite-monochromated Mo radiation (**1** · 2MeCN) and graphite-monochromated Cu radiation (**2**). Complete crystal data and parameters for data collection and processing are reported in Table 1. Unit cell dimensions were determined and refined by using the angular settings of 25 automatically centered reflections in the ranges $11 < 2\vartheta < 23°$ for **1** · 2MeCN and $22 < 2\vartheta < 54°$ for **2**. Three standard reflections monitored every 97 reflections showed less than 3% variation and no decay. Lorentz, polarization and Ψ-scan absorption corrections were applied using Crystal Logic software.

Table 1
Crystallographic data for complexes **1** · 2MeCN and **2**

Parameter	**1** · 2MeCN	**2**
Formula	$C_{94}H_{80}Mn_6N_6O_{25}$	$C_{82}H_{64}Mn_6N_6O_{22}$
Formula weight	2023.44	1815.16
Crystal colour, habit	orange, prism	orange, prism
Crystal dimensions (mm)	0.10 × 0.30 × 0.50	0.12 × 0.15 × 0.45
Crystal system	triclinic	monoclinic
Space group	$P\bar{1}$	$P2_1/a$
Unit cell dimensions		
α (Å)	16.385(8)	20.200(10)
b (Å)	16.422(7)	17.214(9)
c (Å)	20.990(10)	23.449(15)
α (°)	94.10(2)	
β (°)	105.27(2)	90.95(2)
γ (°)	113.81(2)	
V (Å^3)	4883(4)	8153(8)
Z	2	4
$\rho_{calc.}$ (g cm^{-3})	1.376	1.479
Radiation, λ (Å)	Mo Kα, 0.71073	Cu Kα, 1.54180
Temperature (K)	293(2)	293(2)
Scan mode/speed (° min^{-1})	ϑ–2ϑ/1.7	ϑ–2ϑ/1.5
$2\theta_{max}$ (°)	45.8	83.0
μ (mm^{-1})	0.827	7.985
Reflections collected/unique (R_{int})	13920/13358 (0.0216)	5614/5421 (0.0755)
Data with $I > 2\sigma(I)$	9671	4258
Parameters refined	1179	625
$(\Delta\rho)_{max}$, $(\Delta\rho)_{min}$ (e Å^{-3})	0.414, −0.384	0.658, −0.521
Goodness-of-fit (on F^2)	1.040	1.033
R_1,[a] wR_2[b] (all data)	0.0784, 0.1565	0.0964, 0.1988
R_1,[a] wR_2[b] ($I > 2\sigma(I)$)	0.0509, 0.1364	0.0766, 0.1837

[a] $R_1 = \sum(|F_o| - |F_c|)/\sum(|F_o|)$.

[b] $wR_2 = \{\sum[w(F_o^2 - F_c^2)^2]/\sum[w(F_o^2)^2]\}^{1/2}$.

The structures were solved by direct methods using SHELXS-86 [15] and refined by full-matrix least squares techniques on F^2 with SHELXL-97 [16]. For the structure of **1** · 2MeCN, all hydrogen atoms were introduced at calculated positions as riding on bonded atoms and all non-hydrogen atoms were refined using anisotropic thermal parameters, except of the solvent acetonitrile molecules, which were refined isotropically. For **2**, only the metal and the coordinated atoms were refined anisotropically; the rest were refined isotropically. None of the hydrogen atoms were included in the refinement.

3. Results and discussion

3.1. Syntheses

The reactions between $Mn(O_2CPh)_2 \cdot 2H_2O$ and 4hmpH or pym in MeCN gave the complexes $[Mn_6O_2(O_2CPh)_{10}(4hmpH)_3(MeCN)]$ (**1**) and $[Mn_6O_2(O_2CPh)_{10}(pym)_2(MeCN)_2]$ (**2**), respectively; the former was crystallographically identified as **1** · 2MeCN. The complexes are mixed-valent species containing four Mn^{II} and two Mn^{III} ions. Given that the starting manganese source contains only Mn^{II} ions, it is clear that the Mn^{III} ions are formed by aerial oxidation during stirring, as observed by the colour change from pale yellow to dark orange. As is almost always the case in Mn cluster chemistry, the mechanism of formation is likely to be complicated, involving the protonation/deprotonation, oxidation/reduction and structural rearrangement of several species in solution, and thus a detailed mechanistic description is unfeasible.

Complexes **1** and **2** seem to be the only isolable products from the $Mn(O_2CPh)_2 \cdot 2H_2O$/4hmpH and $Mn(O_2CPh)_2 \cdot 2H_2O$/pym reaction systems in MeCN. The Mn^{II} to ligand reaction ratio, the presence/absence of countercations or -anions, and the crystallization method (addition of a precipitation solvent or slow evaporation at room temperature) have no influence on the identity of the products. Thus, despite our efforts we could not obtain anionic or cationic complexes. With the identity of compound **1** established we also tried similar reactions but employing a large excess of $Mn(O_2CPh)_2 \cdot 2H_2O$ (e.g., $Mn(O_2CPh)_2 \cdot 2H_2O$:4hmpH = 4:1) as a means of obtaining complexes containing the deprotonated ligand $4hmp^-$. However, these yielded the known complex $[Mn_6O_2(O_2CPh)_{10}(MeCN)_4]$ [17] and/or non-crystalline materials.

Several approaches leading to the isolation of hexanuclear Mn complexes with the $\{Mn_4^{II}Mn_2^{III}O_2\}^{10+}$ core are known [17–19]. These methods can be divided into four groups. The first one is based on $\mathrm{Mn^{II}(O_2CR)_2}$ oxidation with oxygen [18a–18d], $\mathrm{MnO_4^-}$ [17,18e] or bis(trimethylsilyl)peroxide [18f]. The second involves reduction and subsequent coupling of trinuclear $\{\mathrm{Mn^{II}Mn_2^{III}O}\}^{6+}$ species resulting in formation of the $\{\mathrm{Mn_4^{II}Mn_2^{III}O_2}\}^{10+}$ core. The reducing agents were sodium acenaphthylenide [19a], phenolic molecules [19a] or toluene [19b]. The third method involves construction of the $\{\mathrm{Mn_4^{II}Mn_2^{III}O_2}\}^{10+}$ unit by reduction of a species containing the $\{\mathrm{Mn_4^{III}O_2}\}^{8+}$ core [17] or by a reductive deaggregation (cleavage) of complexes containing the $\{\mathrm{Mn_8^{III}Mn_4^{IV}O_{12}}\}^{16+}$ core [20], the latter being described by the authors as "thermal" decarboxylation. In all of the above-mentioned cases, the carboxylate ions were already present in the Mn starting materials or in the reaction mixtures, and were not involved in any redox process. Recently Quahab, Pavlishchuk and co-workers [21] reported an easy one-pot redox reaction for the preparation of complexes containing the $\{\mathrm{M_4^{II}Mn_2^{III}O_2}\}^{10+}$ core (M = Mn, Co, Ni). The reaction of metal nitrates with benzaldehyde under aerobic conditions results in direct in situ generation of both $\mathrm{Mn^{III}}$ ions and benzoate anions in one step by an oxidation process of $\mathrm{Mn^{II}}$ and benzaldehyde with nitrates.

3.2. Description of structures

The molecular structures of complexes **1** and **2** are depicted in Figs. 2 and 5, respectively. The core of complex **1** is presented in Fig. 3. Selected interatomic distances and angles are listed in Tables 2 and 4, respectively. The molecular structure of complex **2** is similar in many aspects with that of **1** except for terminal ligation and, thus, only the structure of complex **1** will be discussed in detail.

The structure of **1** consists of six Mn ions arranged as two edge-sharing tetrahedra. At the center of each tetrahedron lies a μ_4-$\mathrm{O^{2-}}$ ion. Peripheral ligation is accomplished by 10 bridging benzoate, three terminal 4hmpH and one terminal MeCN groups. Each Mn is six-coordinate and possesses distorted octahedral geometry. Charge considerations indicate a mixed-valence $\mathrm{Mn_4^{II}Mn_2^{III}}$ description, and the $\mathrm{Mn^{III}}$ centers are assigned as central Mn(5) and Mn(6). This is based, primarily, on consideration of the structural parameters and BVS calculations [22] listed in Tables 2 and 3, respectively. Thus, Mn(5,6)–O(101,102) distances (average 1.891 Å) are noticeably shorter than Mn(1,2,3,4)–O(101,102) distances (average 2.211 Å), consistent with the higher oxidation state in the former. Similarly, Mn(5,6)–$\mathrm{O_{carboxylate}}$ distances (average 2.101 Å) are

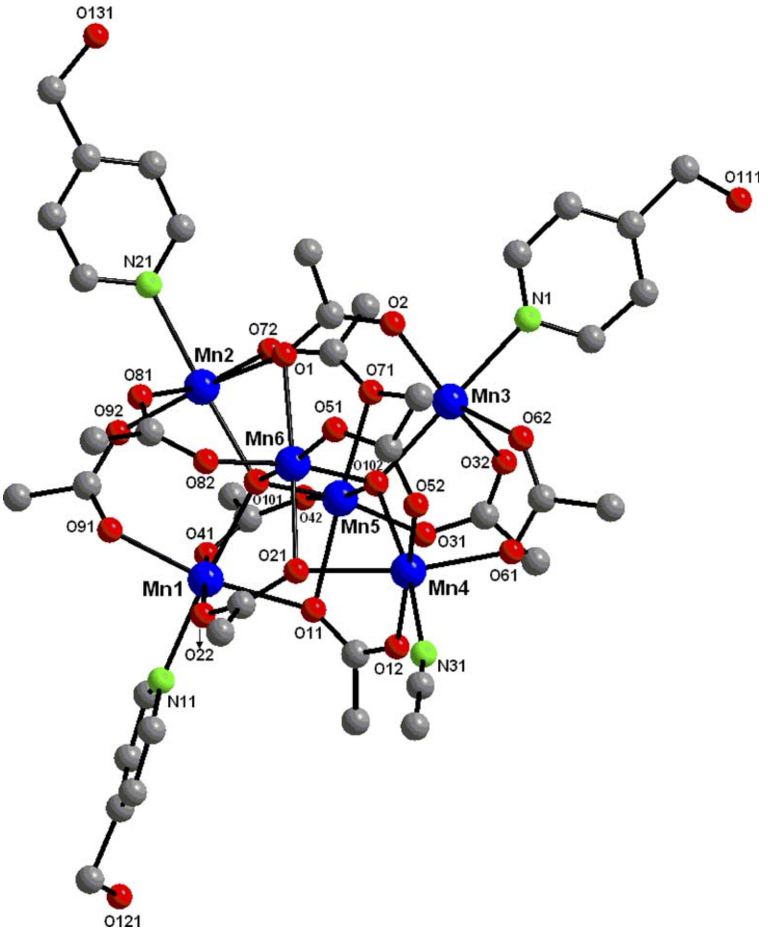

Fig. 2. Partially labelled plot of the hexanuclear molecule of complex **1** · 2MeCN; only the *ipso* carbon atoms of the phenyl groups of the benzoato ligands are shown. The crystal lattice solvents have been omitted for clarity reasons.

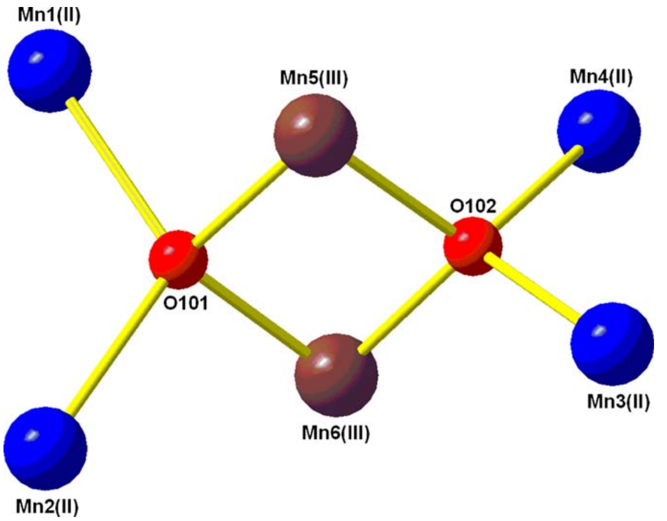

Fig. 3. Ball-and-stick presentation of the $[Mn_4^{II}Mn_2^{III}(\mu_4\text{-}O)_2]^{10+}$ core of **1**.

noticeably shorter than Mn(1,2,3,4)–$O_{carboxylate}$ distances (average 2.179 Å). The Mn^{III} pair is consequently bridged by two μ_4-O^{2-} whereas each $Mn^{II}Mn^{III}$ and $Mn^{II}Mn^{II}$ pair is bridged by only one μ_4-O^{2-}. The 10 benzoate groups separate into two classes. Six are μ_2 with each of their carboxylate oxygen atoms being terminally ligated to a Mn. The other four benzoates are μ_3 with one carboxylate oxygen atom terminally ligated to a Mn^{II}, whereas the other carboxylate oxygen is bridging a $Mn^{II}Mn^{III}$ pair; the latter four oxygen atoms are O(1,11,21,71). The ligated atom of 4hmpH is the pyridyl nitrogen atom. The two Mn^{III} atoms also show the Jahn-Teller distortion expected for an octahedral high-spin d^4 ion, taking the form of an axial elongation with the μ_2-oxygen atoms O(1,11,21,71) of the μ_3 benzoate groups occupying axial positions. Finally each remaining terminal position at the Mn^{II} sites is occupied by either a 4hmpH or the MeCN group. Why partial rather than no complete substitution of solvent MeCN by 4hmpH has occurred is difficult to rationalize.

In addition to the "edge-sharing tetrahedra" description of the Mn_6O_2 core (Fig. 3), two alternative ways of describing it can be presented that emphasize its structural relationship to smaller nuclearity Mn/O units: (i) the Mn_6O_2 unit can be considered as two $[Mn_3O]^{5+}$ units, joined together by each of the μ_3-O^{2-} atoms becoming μ_4 by ligating to the Mn^{III} center of the adjacent Mn_3O unit. The two $[Mn_2^{II}Mn^{III}O]^{5+}$ units comprising the $\{Mn_6O_2\}^{10+}$ core of **1** are Mn(1,2,6)O(101) and Mn(3,4,5)O(102) or, alternatively, Mn(1,2,5)O(101) and Mn(3,4,6)O(102). (ii) The $\{Mn_6O_2\}^{10+}$ core can be considered to contain the $[Mn_2^{II}Mn_2^{III}O_2]$ core of $[Mn_4O_2(O_2CMe)_6(bpy)_2]$ [9a]. The latter possesses a planar Mn_4 rhombus with the two μ_3-O^{2-} bridges, one above and one below the plane.

This unit is to be found within **1** (Mn(1,3,5,6)O(101,102) or Mn(2,4,5,6)O(101,102)), and completion of the Mn_6O_2 core then requires merely the conversion of the two μ_3-O^{2-} to μ_4-O^{2-} by ligation to an additional Mn^{II} center. The "short" $Mn^{III}\ldots Mn^{III}$ (2.817(19) Å) and "long" $Mn^{II}\ldots Mn^{III}$ (3.13–3.57 Å) distances compare favorably with those in $[Mn_4O_2(O_2CMe)_6(bpy)_2]$ (2.779(1) and 3.3–3.5 Å, respectively). Also note that, although the oxidation levels do not correspond, the Mn_6O_2 unit also contains the non-planar "butterfly"-like Mn_4O_2 unit found in $[Mn_4^{III}O_2(O_2CMe)_7(bpy)_2]^+$ [9a]. Such a unit in **1** would be that formed by Mn(1,2,5,6)O(101,102) or Mn(3,4,5,6)O(101,102), with Mn(5,6) representing the "hinge" or "backbone" positions, and completion of Mn_6O_2 again requires conversion of μ_3-O^{2-} to μ_4-O^{2-} by ligation to additional Mn sites. Thus, the planar and butterfly-like Mn_4O_2 units represent the products from two possible ways of removing two Mn atoms from the $\{Mn_6O_2\}^{10+}$ core, as shown in Fig. 4.

The third possibility would yield a $\{Mn_4(\mu_2\text{-}O)(\mu_4\text{-}O)\}^{6+}$ unit; this is currently unknown.

The crystal structure of **1** · 2MeCN is stabilized by a strong intermolecular hydrogen bond. The uncoordinated hydroxyl oxygens O(121) and O(131) are the donor and the acceptor, respectively; its dimensions are: O(121)…O(131) 2.692 Å, HO(121)…O(131) 2.011 Å, O(121)–HO(121)…O(131) 155.5°.

Compound **1** is the third structurally characterized complex of *any* metal containing 4-(hydroxymethyl)pyridine (neutral or anionic) as a ligand. The previously characterized complexes are $[CuCl(4hmpH)_4]Cl$ [23a] and $[Cu(clof)_2(4hmpH)_2(H_2O)] \cdot 2H_2O$ [23b], where $clof^-$ is 2-(4-chlorophenoxy)-2-methylpropionate(−1). In the three complexes the neutral 4hmpH molecule behaves as a N-monodentate ligand.

The structure of complex **2** (Fig. 5) is essentially identical with that of **1** except for two terminal pym and one MeCN groups replacing the three terminal 4hmpH ligands. The partial listing of structural parameters in Table 4

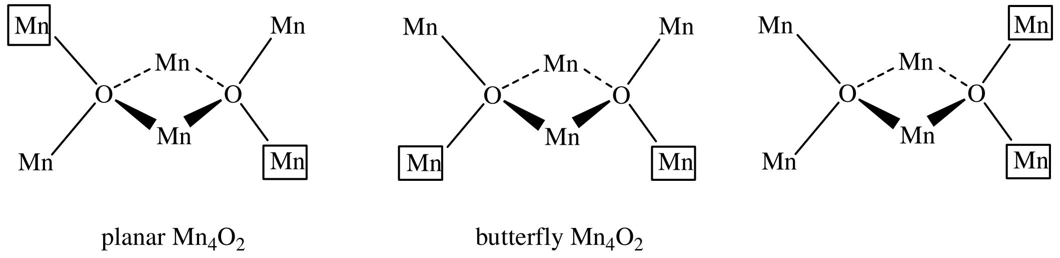

Fig. 4. Three ways of describing the $\{Mn_4^{II}Mn_2^{III}(\mu_4\text{-}O)_2\}^{10+}$ core present in complex **1**.

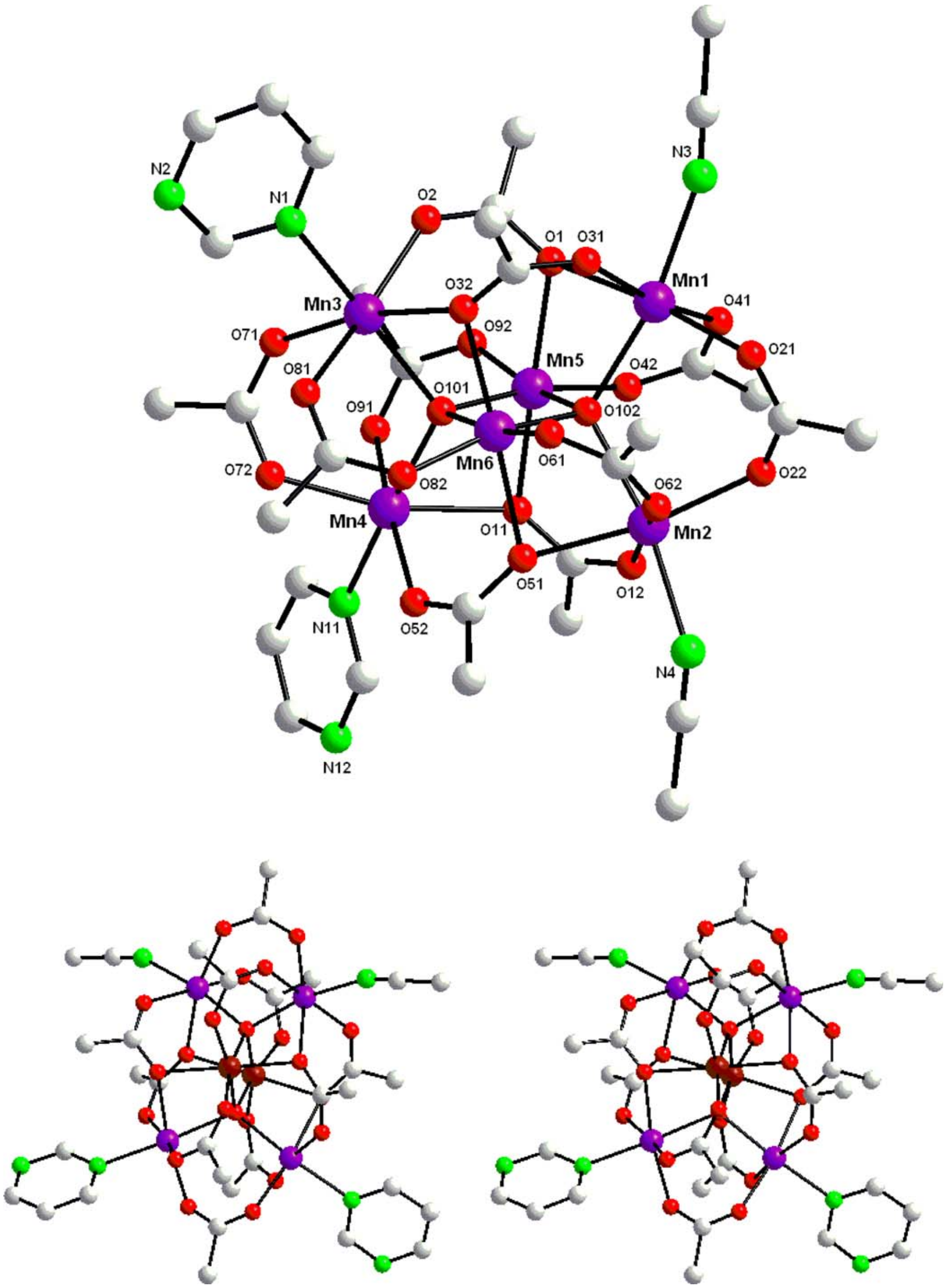

Fig. 5. Partially labelled plot and a stereopair of complex **2**; only the *ipso* carbon atoms of the phenyl groups of the benzoato ligands are shown. Colour code: Mn^{II}, blue; Mn^{III}, brown; O, red; N, green; C, gray (For interpretation of the references to colour in this figure legend, the reader is referred to the web version of this article.).

shows the near congruency of the $\{Mn_6O_2\}^{10+}$ cores of complexes **1** and **2**. The crystal structure of **2** is stabilized by π–π stacking interactions between benzoate ligands of neighboring Mn_6 complexes.

Complex **2** joins a handful of structurally characterized Mn–pym complexes [14]. The previously characterized complexes are $[\{Mn^{II}(pym)(H_2O)\}_2\ \{Mn^{II}(H_2O)_2\}\{W^{V}(CN)_8\}_2]\cdot 2pym\cdot 2H_2O$ [14a], $[Mn^{II}(N_3)_2(pym)]_n$ [14b,c], $[Mn^{II}(hfac)_2(pym)(H_2O)]$ [14d] and $[Mn^{III}(NCS)L(pym)]$ [14e], where $hfac^-$ is hexafluoroacetylacetonate and L is the tetradentate chelating ligand *N*,*N*′-ethylenebis(1-phenyl-3-imino-1-butanonate)(−2). In these complexes pym adopts either the monodentate [14d,14e] or the bidentate bridging [14a,14b,14c] coordination mode.

Complexes **1** and **2** extend to seven the number [17,18e,19a,21] of structurally characterized complexes $[Mn^{II}_4Mn^{III}_2O_2(O_2CPh)_{10}L_4]$ and $[Mn^{II}_4Mn^{III}_2O_2(O_2CPh)_{10}L_xL'_y]$, where L,L′ are monodentate ligands and $x + y = 4$

Table 2
Selected interatomic distances (Å) and bond angles (°) for complex **1** · 2MeCN

Interatomic distances			
Mn(1)…Mn(2)	3.802(51)	Mn(2)–N(21)	2.293(4)
Mn(1)…Mn(3)	6.048(48)	Mn(3)–O(102)	2.217(3)
Mn(1)…Mn(4)	4.748(63)	Mn(3)–O(2)	2.121(4)
Mn(1)…Mn(5)	3.133(2)	Mn(3)–O(32)	2.163(4)
Mn(1)…Mn(6)	3.577(72)	Mn(3)–O(62)	2.131(4)
Mn(2)…Mn(3)	4.994(48)	Mn(3)–O(71)	2.380(4)
Mn(2)…Mn(4)	6.004(54)	Mn(3)–N(1)	2.290(5)
Mn(2)…Mn(5)	3.536(20)	Mn(4)–O(102)	2.215(3)
Mn(2)…Mn(6)	3.158(2)	Mn(4)–O(12)	2.117(4)
Mn(3)…Mn(4)	3.806(39)	Mn(4)–O(21)	2.252(3)
Mn(3)…Mn(5)	3.188(2)	Mn(4)–O(52)	2.153(4)
Mn(3)…Mn(6)	3.572(17)	Mn(4)–O(61)	2.101(4)
Mn(4)…Mn(5)	3.549(19)	Mn(4)–N(31)	2.261(5)
Mn(4)…Mn(6)	3.136(2)	Mn(5)–O(101)	1.890(3)
Mn(5)…Mn(6)	2.817(19)	Mn(5)–O(102)	1.888(3)
Mn(1)–O(101)	2.219(3)	Mn(5)–O(11)	2.275(3)
Mn(1)–O(11)	2.232(3)	Mn(5)–O(31)	1.953(3)
Mn(1)–O(22)	2.124(4)	Mn(5)–O(42)	1.955(4)
Mn(1)–O(41)	2.168(4)	Mn(5)–O(71)	2.230(3)
Mn(1)–O(91)	2.134(4)	Mn(6)–O(101)	1.895(3)
Mn(1)–N(11)	2.279(5)	Mn(6)–O(102)	1.889(3)
Mn(2)–O(101)	2.192(3)	Mn(6)–O(1)	2.236(3)
Mn(2)–O(1)	2.331(3)	Mn(6)–O(21)	2.247(3)
Mn(2)–O(72)	2.130(3)	Mn(6)–O(51)	1.951(3)
Mn(2)–O(81)	2.146(3)	Mn(6)–O(82)	1.957(3)
Mn(2)–O(92)	2.177(4)		
Bond angles			
Mn(1)–O(101)–Mn(2)	119.0(1)	O(2)–Mn(3)–O(32)	162.7(2)
Mn(1)–O(101)–Mn(5)	99.0(1)	O(2)–Mn(3)–O(102)	93.8(1)
Mn(1)–O(101)–Mn(6)	120.6(1)	O(2)–Mn(3)–N(1)	85.9(2)
Mn(2)–O(101)–Mn(5)	119.9(1)	O(62)–Mn(3)–O(71)	164.2(1)
Mn(2)–O(101)–Mn(6)	101.0(1)	O(62)–Mn(3)–N(1)	86.4(2)
Mn(5)–O(101)–Mn(6)	96.2(1)	O(102)–Mn(3)–N(1)	178.4(2)
Mn(3)–O(102)–Mn(4)	118.3(1)	O(12)–Mn(4)–O(21)	90.4(2)
Mn(3)–O(102)–Mn(5)	101.6(1)	O(12)–Mn(4)–O(52)	171.3(2)
Mn(3)–O(102)–Mn(6)	120.7(2)	O(21)–Mn(4)–O(61)	169.8(2)
Mn(4)–O(102)–Mn(5)	119.6(2)	O(21)–Mn(4)–N(31)	91.0(2)
Mn(4)–O(102)–Mn(6)	99.3(1)	O(61)–Mn(4)–O(52)	87.2(2)
Mn(5)–O(102)–Mn(6)	96.5(1)	O(102)–Mn(4)–N(31)	168.4(2)
O(11)–Mn(1)–O(22)	92.1(1)	O(11)–Mn(5)–O(42)	89.8(1)
O(11)–Mn(1)–O(41)	86.9(1)	O(11)–Mn(5)–O(71)	172.2(1)
O(11)–Mn(1)–O(91)	167.8(1)	O(31)–Mn(5)–O(71)	91.8(1)
O(11)–Mn(1)–N(11)	95.9(2)	O(31)–Mn(5)–O(101)	168.4(1)
O(22)–Mn(1)–O(41)	173.6(2)	O(31)–Mn(5)–O(102)	95.4(1)
O(101)–Mn(1)–N(11)	173.8(2)	O(42)–Mn(5)–O(102)	170.4(1)
O(1)–Mn(2)–O(72)	85.8(1)	O(1)–Mn(6)–O(21)	174.3(1)
O(1)–Mn(2)–O(81)	83.2(1)	O(1)–Mn(6)–O(82)	91.8(1)
O(1)–Mn(2)–O(92)	167.2(1)	O(21)–Mn(6)–O(51)	91.9(1)
O(72)–Mn(2)–O(81)	163.8(2)	O(51)–Mn(6)–O(101)	169.4(1)
O(92)–Mn(2)–N(21)	88.8(2)	O(51)–Mn(6)–O(102)	94.2(1)
O(101)–Mn(2)–N(21)	173.6(1)	O(82)–Mn(6)–O(102)	169.7(1)

or 5. These complexes contain the $\{Mn^{II}_4Mn^{III}_2(\mu_4\text{-O})_2\}^{10+}$ core (see Fig. 3). Rather than discuss similarities, we list in Table 5 comparative structural parameters concerning the core of the benzoate clusters. The remarkable similarity of the cores is clearly evident. Obviously, the nature of the terminal ligands L,L′ has very little structural effect.

It should be mentioned at this point that two other hexanuclear Mn clusters possessing a Mn_6O_2 unit have been structurally characterized [24,25]; however, the metal

Table 3
Bond valence sum[a,b] (BVS) calculations for the Mn and selected oxygen atoms in **1**

Atom	Mn^{II}	Mn^{III}	Mn^{IV}
Mn(1)	$\underline{2.101}$	1.822	1.886
Mn(2)	$\underline{2.014}$	1.746	1.807
Mn(3)	$\underline{2.002}$	1.738	1.798
Mn(4)	$\underline{2.161}$	1.877	1.941
Mn(5)	3.167	$\underline{3.126}$	3.042
Mn(6)	3.171	$\underline{3.128}$	3.045

	BVS	assignment
O(101)	2.048	O^{2-}
O(102)	2.044	O^{2-}

[a] The underlined value is the one closest to the charge for which it was calculated. The oxidation state of a particular atom can be taken as the nearest whole number to the underlined value.

[b] The O atom is not protonated if the BVS is ~2, it is monoprotonated if

Table 4
Selected interatomic distances (Å) and bond angles (°) for complex **2**

Interatomic distances			
Mn(1)…Mn(2)	3.769(21)	Mn(2)–N(4)	2.274(11)
Mn(1)…Mn(3)	4.920(4)	Mn(3)–O(101)	2.182(7)
Mn(1)…Mn(4)	6.037(4)	Mn(3)–O(2)	2.108(9)
Mn(1)…Mn(5)	3.150(3)	Mn(3)–O(32)	2.333(8)
Mn(1)…Mn(6)	3.560(21)	Mn(3)–O(71)	2.104(8)
Mn(2)…Mn(3)	5.994(6)	Mn(3)–O(81)	2.171(9)
Mn(2)…Mn(4)	4.847(5)	Mn(3)–N(1)	2.252(10)
Mn(2)…Mn(5)	3.564(19)	Mn(4)–O(101)	2.202(7)
Mn(2)…Mn(6)	3.142(3)	Mn(4)–O(11)	2.270(8)
Mn(3)…Mn(4)	3.758(16)	Mn(4)–O(52)	2.153(8)
Mn(3)…Mn(5)	3.510(14)	Mn(4)–O(72)	2.120(8)
Mn(3)…Mn(6)	3.144(3)	Mn(4)–O(91)	2.201(8)
Mn(4)…Mn(5)	3.164(3)	Mn(4)–N(11)	2.277(10)
Mn(4)…Mn(6)	3.573(24)	Mn(5)–O(101)	1.894(8)
Mn(5)…Mn(6)	2.823(3)	Mn(5)–O(102)	1.907(8)
Mn(1)–O(102)	2.192(7)	Mn(5)–O(1)	2.239(8)
Mn(1)–O(1)	2.315(8)	Mn(5)–O(11)	2.219(8)
Mn(1)–O(21)	2.125(9)	Mn(5)–O(42)	1.961(8)
Mn(1)–O(31)	2.127(8)	Mn(5)–O(92)	1.949(9)
Mn(1)–O(41)	2.149(9)	Mn(6)–O(101)	1.894(8)
Mn(1)–N(3)	2.268(11)	Mn(6)–O(102)	1.899(8)
Mn(2)–O(102)	2.193(7)	Mn(6)–O(32)	2.211(8)
Mn(2)–O(12)	2.136(9)	Mn(6)–O(51)	2.232(8)
Mn(2)–O(22)	2.106(8)	Mn(6)–O(62)	1.942(9)
Mn(2)–O(51)	2.245(8)	Mn(6)–O(82)	1.961(8)
Mn(2)–O(61)	2.174(9)		
Bond angles			
Mn(1)–O(102)–Mn(2)	118.5(3)	O(12)–Mn(2)–O(61)	168.2(3)
Mn(1)–O(102)–Mn(5)	100.2(3)	O(22)–Mn(2)–O(51)	166.5(3)
Mn(1)–O(102)–Mn(6)	120.8(3)	O(102)–Mn(2)–N(4)	168.6(4)
Mn(2)–O(102)–Mn(5)	120.6(3)	O(2)–Mn(3)–O(81)	165.1(3)
Mn(2)–O(102)–Mn(6)	100.1(3)	O(32)–Mn(3)–O(71)	168.5(3)
Mn(5)–O(102)–Mn(6)	95.8(3)	O(101)–Mn(3)–N(1)	168.5(4)
Mn(3)–O(101)–Mn(4)	118.0(3)	O(11)–Mn(4)–O(72)	164.5(3)
Mn(3)–O(101)–Mn(5)	118.7(3)	O(52)–Mn(4)–O(91)	167.1(3)
Mn(3)–O(101)–Mn(6)	100.7(3)	O(101)–Mn(4)–N(11)	172.6(3)
Mn(4)–O(101)–Mn(5)	100.9(3)	O(1)–Mn(5)–O(11)	172.5(3)
Mn(4)–O(101)–Mn(6)	121.3(4)	O(42)–Mn(5)–O(101)	168.9(3)
Mn(5)–O(101)–Mn(6)	96.4(3)	O(92)–Mn(5)–O(102)	167.8(3)
O(1)–Mn(1)–O(21)	170.3(3)	O(32)–Mn(6)–O(51)	174.0(3)
O(31)–Mn(1)–O(41)	169.3(3)	O(62)–Mn(6)–O(101)	171.2(3)
O(102)–Mn(1)–N(3)	167.5(4)	O(82)–Mn(6)–O(102)	167.2(3)

Table 5
Selected structural parameters for the $\{Mn^{II}_4Mn^{III}_2(\mu_4\text{-}O)_2\}^{10+}$ cores present in the structurally characterized $[Mn_6O_2(O_2CPh)_{10}L_4]$ and $[Mn_6O_2(O_2CPh)_{10}L_xL'_y]$ complexes ($x + y = 4$ or 5)

Complex[a]	$Mn^{III}\ldots Mn^{III}$ (Å)	Mn^{III}–O_{oxo}[b] (Å)	Mn^{II}–O_{oxo}[b] (Å)	Mn^{III}–O_{oxo}–Mn^{III}[b] (°)	Ref.
$[Mn_6O_2(O_2CPh)_{10}(py)_2(MeCN)_2]$	2.820	1.888	2.196	96.7	[19a]
$[Mn_6O_2(O_2CPh)_{10}(py)_4]$	2.805	1.897	2.208	95.4	[19a]
$[Mn_6O_2(O_2CPh)_{10}(MeCN)_4]$	2.807	1.889	2.195	96.0	[17]
$[Mn_6O_2(O_2CPh)_{10}(EtOH)_4(H_2O)]$	2.802	1.890	2.213	95.7	[18a]
$[Mn_6O_2(O_2CPh)_{10}(DMF)_4]$	2.810	1.892	2.200	96.0	[21]
$[Mn_6O_2(O_2CPh)_{10}(4hmpH)_3(MeCN)]$	2.817	1.891	2.211	96.4	this work
$[Mn_6O_2(O_2CPh)_{10}(pym)_2(MeCN)_2]$	2.823	1.899	2.192	96.1	this work

[a] Solvate molecules have been omitted.
[b] Mean values.

oxidation levels are different compared with those in **1** and **2**. Complex $[Mn_6O_2(O_2CPh)_{12}(py)_2]$, isolated using solvothermal techniques, contains the $\{Mn^{II}_2Mn^{III}_4(\mu_3\text{-}O)_2\}^{12+}$ core [24], and complex $[Mn_6O_2(O_2CPh)_8(O_3PPh)_2(O_2PHPh)_2(py)_2]$ has the $\{Mn^{III}_6(\mu_3\text{-}O)_2\}^{14+}$ core [25].

3.3. IR spectra

A characteristic feature in the IR spectrum of **1** is the appearance of a medium broad band at ~3415 cm^{-1} assignable to the ν(OH) vibration of 4hmpH [23a]. Several bands appear in the 1610–1390 cm^{-1} range in the spectra of **1** and **2**. Contributions from the benzoate $\nu_{as}(CO_2)$ and $\nu_s(CO_2)$ modes would be expected in this region, but overlap with the stretching vibrations of the aromatic rings, $\delta(CH_2)$ (for **1**) and $\delta(CH_3)$ renders assignments tentative and application of the spectroscopic criterion of Deacon and Phillips [26] difficult. The strong bands at 1563 (**1**), 1568 (**2**) and 1400 (**1**), 1396 (**2**) cm^{-1} have $\nu_{as}(CO_2)$ and $\nu_s(CO_2)$ characters [24], respectively. The difference Δ ($\Delta = \nu_{as}(CO_2) - \nu_s(CO_2)$) is 163 cm^{-1} for **1** and 172 cm^{-1} for **2**, less than that for NaO_2CPh (184 cm^{-1}), as expected for the bridging modes of benzoate ligation [26].

A medium-intensity band at 610 (**1**) and 607 (**2**) cm^{-1} is tentatively assigned to a vibration involving a Mn^{III}–O^{2-} stretch [27].

3.4. Magnetochemistry

Direct current magnetic susceptibility data were collected in the 5.00–300 K range on powdered microcrystalline samples of **1** and **2** restrained in eicosane to prevent torquing. The χ_mT versus T data for complex **1** are shown in Fig. 6. Very similar behaviour was observed, with the χ_mT decreasing from 17.41 and 16.60 cm^3 mol^{-1} K at 300 K to 1.21 and 0.98 cm^3 mol^{-1} K at 5.00 K for **1** and **2**, respectively. The rate of decrease increases below ~50 K. The room temperature χ_mT values are less than the 23.5 cm^3 mol^{-1} K spin-only value ($g = 2.0$) expected for a $4Mn^{II}$, $2Mn^{III}$ complex with non-interacting centres, indicating the presence of appreciable antiferromagnetic interactions between the Mn ions. The χ_mT versus T data for both complexes appear to be heading for 0 at 0 K and suggest an $S_T = 0$ ground state. Because the complex contains multiple Mn^{II} ions that are known to promote weak exchange interactions, clear identification of the ground state by magnetization versus field data would be precluded by the low-lying excited states crossing with the ground state in the applied fields of several Tesla. Thus, the ac susceptibility technique was employed [28]. Like the dc data, the ac data, collected in the temperature range 1.8–10 K, are very similar for the two complexes. In addition, they are essentially superimposable with the dc data, except at the very lowest temperatures. Extrapolation of the $\chi_m'T$ signal from values above ~3 K (to avoid decreases due to intermolecular interactions at lower temperatures) to 0 K gives a value of <0.3 cm^3 mol^{-1} K, suggesting an $S_T = 0$ ground state for both complexes.

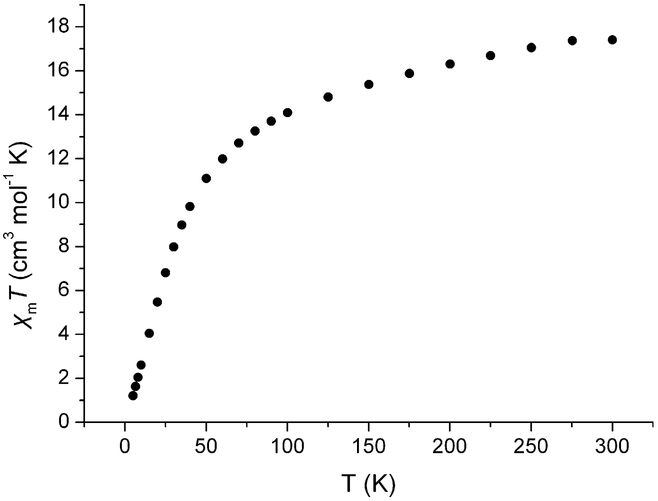

Fig. 6. Plot of χ_mT vs T for **1**. χ_m is the dc magnetic susceptibility measured in a 1 kG field.

The $S_T = 0$ ground state indicated for **1** and **2** is not surprising given its structural similarity to the family of previous hexanuclear compounds containing the $\{Mn^{II}_4Mn^{III}_2(\mu_4\text{-}O)_2\}^{10+}$ core, which have been found to have $S_T = 0$ [19a,21]. Since typically $Mn^{II}\ldots Mn^{II}$ and $Mn^{II}\ldots Mn^{III}$ exchange interactions are weak and antiferromagnetic [29], the apparent $S_T = 0$ ground state of **1** and **2** seems to be a consequence of the well established [19a,21] strong antiferromagnetic coupling at the central

$Mn_2^{III}O_2$ unit of the molecules. This strong, dominating coupling will give an $S_T = 0$ ground state for the complete molecules [19a,30].

We refrain from fitting the magnetic data of **1** and **2**, since detailed studies are available for structurally similar $Mn_4^{II}Mn_2^{III}$ complexes. For example, the results of the solid-state magnetic susceptibility data for complex $[Mn_6O_2(O_2CPh)_{10}(py)_2(MeCN)_2]$ in the temperature range 3.0–300 K were reported [19a]. With use of the idealized symmetry of two edge-sharing tetrahedra (D_{2h}), the derivation by the Kambe vector-coupling method [31] of a theoretical model to account for the intramolecular exchange interactions was described. Least-squares fitting of the susceptibility versus temperature data to the model yielded the parameters $J_1 = -42.0\ cm^{-1}$, $J_2 = -0.8\ cm^{-1}$, $J_3 = -2.4\ cm^{-1}$ and $g = 1.90$, where the J values refer to the $Mn^{III}\ldots Mn^{III}$, $Mn^{II}\ldots Mn^{III}$ and $Mn^{II}\ldots Mn^{II}$ exchange interactions, respectively (spin Hamiltonian for a pair being $H = -2J_{AB}S_A \cdot S_B$) [19a]. These exchange parameters give an $S_T = 0$ ground state with two degenerate $S_T = 1$ states at $4\ cm^{-1}$ and degenerate $S_T = 0, 1, 2$ states at $9\ cm^{-1}$ higher in energy. Using the same model (idealized symmetry D_{2h}), Quahab, Pavlischuk and co-workers reported recently [21] the values $J_1 = -50.5\ cm^{-1}$, $J_2 = -4.2\ cm^{-1}$, $J_3 = -2.1\ cm^{-1}$ and $g = 1.99$ for complex $[Mn_6O_2(O_2CPh)_{10}(DMF)_4]$. There is a good agreement in the J values between the two complexes.

4. Conclusions and perspectives

The initial use of 4hmpH and pym in Mn carboxylate chemistry has provided access to two new hexanuclear, mixed-valence Mn clusters with the $\{Mn_4^{II}Mn_2^{III}(\mu_4\text{-}O)_2\}^{10+}$ core. The two complexes are valuable additions to the chemistry of hexanuclear Mn clusters that contain a Mn_6O_2 unit. This is available at the $Mn_4^{II}Mn_2^{III}$, $Mn_2^{II}Mn_4^{III}$ and Mn_6^{III} levels. Although clusters **1** and **2** have been found to possess an $S_T = 0$ ground state, the potentially bridging modes of 4hmpH or $4hmp^-$ and pym (which have not been realized in the present work) would undoubtedly give Mn_x products structurally different from **1** and **2** and which may have high-spin ground states. In addition, the MeCN terminal ligands present in **1** and **2** could have future utility as sites for facile incorporation of other monodentate ligands by metathesis or as a means of accessing higher-nuclearity species by using bis(monodentate) bridging aromatic heterocycles. Finally, since the intended bridging behaviour of the ligands used has not been achieved in **1** and **2**, we are continuing our synthetic efforts to realise the μ_2/μ_3 potential of the deprotonated 4hmpH ligand and the μ_2 potential of pym in Mn carboxylate chemistry.

Acknowledgments

Th.C.S. and S.P.P. thank European Social Fund (ESF), Operational Program for Educational and Vocational Training II (EPEAEK II), and particularly the Program PYTHAGORAS (Grant b.365.037), for funding the above work. G.C. thanks the National science foundation (CHE-0414155). C.S.P. and A.J.T. thank the European Commission for providing a Marie Curie Grant (HPMT-CT-2001-00421) that enabled the stay of Th.C.S. at the University of Cyprus.

Appendix A. Supplementary data

Crystallographic data in CIF format have been deposited at the Cambridge Crystallographic Data Centre with CCDC Nos. 285383 ($\mathbf{1} \cdot 2MeCN$) and 285384 (**2**). Copies of this information may be obtained free of charge from The Director, CCDC, 12 Union Road, Cambridge, CB2 1EZ, UK (fax: +44 1223 336033; e-mail: deposit@ccdc.cam.ac.uk or http://www.ccdc.cam.ac.uk). Supplementary data associated with this article can be found, in the online version, at doi:10.1016/j.poly.2005.11.019.

References

[1] (a) K.N. Ferreira, T.M. Iverson, K. Maghlaoui, J. Barber, S. Iwata, Science 303 (2004) 1831;
(b) T.G. Carrell, A.M. Tyryshkin, G.C. Dismukes, J. Biol. Inorg. Chem. 7 (2002) 2;
(c) A. Mishra, W. Wernsdorfer, K.A. Abboud, G. Christou, Chem. Commun. (2005) 54.

[2] E.K. Brechin, E.C. Sañudo, W. Wernsdorfer, C. Boskovic, J. Yoo, D.N. Hendrickson, A. Yamaguchi, H. Ishimoto, T.E. Concolino, A.L. Rheingold, G. Christou, Inorg. Chem. 44 (2005) 502.

[3] (a) For reviews, see: G. Christou, D. Gatteschi, D.N. Hendrickson, MRS Bull. 25 (2000) 66;
(b) D. Gatteschi, R. Sessoli, Angew. Chem., Int. Ed. 42 (2003) 268.

[4] (a) Recent literature: N.E. Chakov, M. Soler, W. Wernsdorfer, K.A. Abboud, G. Christou, Inorg. Chem. 44 (2005) 5304;
(b) S. Maheswaran, G. Chastanet, S.J. Teat, T. Mallah, R. Sessoli, W. Wernsdorfer, R.E.P. Winpenny, Angew. Chem., Int. Ed. 44 (2005) 5044;
(c) M. Murugesu, J. Raftery, W. Wernsdorfer, G. Christou, E.K. Brechin, Inorg. Chem. 43 (2004) 4203;
(d) P. King, W. Wernsdorfer, K.A. Abboud, G. Christou, Inorg. Chem. 43 (2004) 7315;
(e) E.C. Sañudo, W. Wernsdorfer, K.A. Abboud, G. Christou, Inorg. Chem. 43 (2004) 4137;
(f) A.J. Tasiopoulos, A. Vinslava, W. Wernsdorfer, K.A. Abboud, G. Christou, Angew. Chem., Int. Ed. 43 (2004) 2117;
(g) M. Soler, W. Wernsdorfer, K. Folting, M. Pink, G. Christou, J. Am. Chem. Soc. 126 (2004) 2156;
(h) H. Zhao, C.P. Berlinguette, J. Basca, A.V. Prosvirin, J.K. Bera, S.E. Tichy, E.J. Schelter, K.R. Dunbar, Inorg. Chem. 43 (2004) 1359;
(i) L.M. Wittick, K.S. Murray, B. Moubaraki, S.R. Batten, L. Spiccia, J.K. Berry, Dalton Trans. (2004) 1003;
(j) C.J. Milios, C.P. Raptopoulou, A. Terzis, F. Lloret, R. Vicente, S.P. Perlepes, A. Escuer, Angew. Chem., Int. Ed. 43 (2004) 210.

[5] For a mini-review describing the available synthetic procedures to Mn SMMs, see: G. Christou, Polyhedron 24 (2005) 2065.

[6] G. Aromi, S.M.J. Aubin, M.A. Bolcar, G. Christou, H.J. Eppley, K. Folting, D.N. Hendrickson, J.C. Huffman, R.C. Squire, H.-L. Tsai, S. Wang, M.W. Wemple, Polyhedron 17 (1998) 3005, and references therein.

[7] J.B. Vincent, H.-R. Chang, K. Folting, J.C. Huffman, G. Christou, D.N. Hendrickson, J. Am. Chem. Soc. 109 (1987) 5703.

[8] M.W. Wemple, H.-L. Tsai, S. Wang, J.P. Claude, W.E. Streib, J.C. Huffman, D.N. Hendrickson, G. Christou, Inorg. Chem. 35 (1996) 6437.

[9] (a) For example, see: J.B. Vincent, C. Christmas, H.-R. Chang, Q. Li, P.D.W. Boyd, J.C. Huffman, D.N. Hendrickson, G. Christou, J. Am. Chem. Soc. 111 (1989) 2086;
(b) A.J. Tasiopoulos, K.A. Abboud, G. Christou, Chem. Commun. (2003) 580.

[10] E. Libby, J.K. McCusker, E.A. Schmitt, K. Folting, D.N. Hendrickson, G. Christou, Inorg. Chem. 30 (1991) 3486.

[11] (a) For example, see: S. Wang, H.-L. Tsai, E. Libby, K. Folting, W.E. Streib, D.N. Hendrickson, G. Christou, Inorg. Chem. 35 (1996) 7578;
(b) G. Aromi, M.J. Knapp, J.-P. Claude, J.C. Huffman, D.N. Hendrickson, G. Christou, J. Am. Chem. Soc. 121 (1999) 5489.

[12] (a) S. Wang, H.-L. Tsai, K. Folting, J.D. Martin, D.N. Hendrickson, G. Christou, J. Chem. Soc., Chem. Commun. (1994) 671;
(b) H.J. Eppley, N. deVries, S. Wang, S.M. Aubin, H.-L. Tsai, K. Folting, D.N. Hendrickson, G. Christou, Inorg. Chim. Acta 263 (1997) 323.

[13] (a) N.C. Harden, M.A. Bolcar, W. Wernsdorfer, K.A. Abboud, W.E. Streib, G. Christou, Inorg. Chem. 42 (2003) 7067;
(b) C. Boskovic, E.K. Brechin, W.E. Streib, K. Folting, J.C. Bollinger, D.N. Hendrickson, G. Christou, J. Am. Chem. Soc. 124 (2002) 3725;
(c) A. Bhattacharjee, Y. Miyazaki, M. Nakano, J. Yoo, G. Christou, D.N. Hendrickson, M. Sorai, Polyhedron 20 (2001) 1607.

[14] (a) T. Kashiwagi, S. Ohkoshi, H. Seino, Y. Mizobe, K. Hashimoto, J. Am. Chem. Soc. 126 (2004) 5024;
(b) A. Escuer, R. Vicente, F.A. Mautner, M.A.S. Goher, M.A.M. Abu-Youssef, Chem. Commun. (2002) 64;
(c) Y. Doi, T. Ishida, T. Nogami, Bull. Chem. Soc. Jpn. 75 (2002) 2455;
(d) D.-M. Hong, H.-H. Wei, K.-H. Chang, G.-H. Lee, Y. Wang, Polyhedron 17 (1998) 3565;
(e) F. Yun-Long, L. Shi-Xiong, Chin. J. Struct. Chem. 15 (1996) 47.

[15] G.M. Sheldrick, SHELXS-86, Structure Solving Program, University of Göttingen, Germany, 1986.

[16] G.M. Sheldrick, SHELXL-97, Program for the Refinement of Crystal Structures from Diffraction Data, University of Göttingen, Germany, 1997.

[17] M.A. Halcrow, W.E. Streib, K. Folting, G. Christou, Acta Crystallogr., Sect. C 51 (1995) 1263.

[18] (a) M. Murie, S. Parsons, R.E.P. Winpenny, J. Chem. Soc., Dalton Trans. (1998) 1423;
(b) P. Karsten, J. Strähle, Acta Crystallogr., Sect. C 54 (1998) 1403;
(c) A.R.E. Baikie, A.J. Howes, M.B. Hursthouse, A.B. Quick, P. Thornton, J. Chem. Soc., Chem. Commun. (1986) 1587;
(d) A.S. Batsanov, Y.T. Struchkov, G.A. Timco, N.V. Gerbeleu, O.S. Manole, S.V. Grebenko, Russ. J. Coord. Chem. 20 (1994) 604;
(e) A.G. Blackman, J.C. Huffman, E.B. Lobkovsky, G. Christou, Polyhedron 11 (1992) 251;
(f) K. Köhler, H.W. Roesky, M. Noltemeyer, H.-G. Schmidt, C. Freire-Erdbrügger, G.M. Sheldrick, Chem. Ber. 126 (1993) 921.

[19] (a) A.R. Schake, J.B. Vincent, Q. Li, P.D.W. Boyd, K. Folting, J.C. Huffman, D.N. Hendrickson, G. Christou, Inorg. Chem. 28 (1989) 1915;
(b) J. Kim, H. Cho, Inorg. Chem. Commun. 7 (2004) 122.

[20] P. Gerbier, D. Ruiz-Molina, J. Gómez, K. Wurst, J. Veciana, Polyhedron 22 (2003) 1951.

[21] K.S. Gavrilenko, S.V. Punin, O. Cador, S. Golhen, L. Quahab, V.V. Pavlishchuk, Inorg. Chem. 44 (2005) 5903.

[22] (a) G.J. Palenik, Inorg. Chem. 36 (1997) 122;
(b) H.H. Thorp, Inorg. Chem. 37 (1998) 5690.

[23] (a) J. Moncol, B. Kalinakova, J. Svorec, M. Kleinova, M. Koman, D. Hudecova, M. Melnik, M. Mazur, M. Valko, Inorg. Chim. Acta 357 (2004) 3211;
(b) J. Moncol, M. Mudra, P. Lonnecke, M. Koman, M. Melnik, J. Chem. Crystallogr. 34 (2004) 423.

[24] D.M. Low, E.K. Brechin, M. Helliwell, T. Mallah, E. Riviére, E.J.L. McInnes, Chem. Commun. (2003) 2330.

[25] E.K. Brechin, R.A. Coxall, A. Parkin, S. Parsons, P.A. Tasker, R.E.P. Winpenny, Angew. Chem., Int. Ed. 40 (2001) 2700.

[26] G.B. Deacon, R.J. Phillips, Coord. Chem. Rev. 33 (1980) 227.

[27] (a) R.D. Cannon, R.P. White, Prog. Inorg. Chem. 36 (1988) 195;
(b) C.J. Milios, Th.C. Stamatatos, P. Kyritsis, A. Terzis, C.P. Raptopoulou, R. Vicente, A. Escuer, S.P. Perlepes, Eur. J. Inorg. Chem. (2004) 2885.

[28] E.C. Sañudo, V.A. Grillo, M.J. Knapp, J.C. Bollinger, J.C. Huffman, D.N. Hendrickson, G. Christou, Inorg. Chem. 41 (2002) 2441, and references therein.

[29] L. Que, A.E. True, Prog. Inorg. Chem. 38 (1990) 97.

[30] C. Boskovic, W. Wernsdorfer, K. Folting, J.C. Huffman, D.N. Hendrickson, G. Christou, Inorg. Chem. 41 (2002) 5107.

[31] K. Kambe, J. Phys. Soc. Jpn. 5 (1950) 48.